Available online at www.sciencedirect.com
ScienceDirect
Physica C 456 (2007) 188–195
PHYSICA C
www.elsevier.com/locate/physc

Review

MgB_2 tunnel junctions and SQUIDs

A. Brinkman [a,*], J.M. Rowell [b]

[a] Faculty of Science and Technology and MESA+, Institute for Nanotechnology, University of Twente, The Netherlands
[b] School of Materials, Arizona State University, Tempe, USA

Received 12 December 2006; accepted 28 January 2007
Available online 7 February 2007

Abstract

Recent advances in the realization and understanding of MgB_2 tunnel junctions and SQUIDs are surveyed. High quality MgB_2 junctions with suitable tunnel barriers have been realized based on both oriented and epitaxial thin MgB_2 films. Multiband transport properties, such as the existence of two energy gaps, phonon spectra and anisotropy have been investigated with these junctions. We review the suitability of different barrier materials and recent advances in obtaining reproducible all-MgB_2 Josephson junctions for superconducting electronic circuitry. The development of epitaxial thin films has also led to high-quality multiband MgB_2 SQUIDs and magnetometers that operate at high temperatures. The multiband nature of MgB_2 provides new phenomena such as the Leggett mode. Manipulating the different phases of the condensates could lead to novel MgB_2 devices with phase degrees of freedom.

PACS: 74.50.+r; 85.25.−j; 74.70.Ad

Keywords: MgB_2; Tunnel junction; SQUID

Contents

1. Introduction

After the discovery of superconductivity in MgB_2 [1], very fast initial progress was made in the realization of thin films, junctions and SQUIDs. Within a couple of months, multilayer MgB_2 Josephson junctions [2] and

* Corresponding author. Tel.: +31 53 489 3122; fax: +31 53 489 1099.
E-mail address: a.brinkman@utwente.nl (A. Brinkman).

0921-4534/$ - see front matter © 2007 Elsevier B.V. All rights reserved.
doi:10.1016/j.physc.2007.01.019

MgB_2 SQUIDs [3] had been realized. This large initial research effort was motivated by the opportunities that MgB_2 gives to applications.

First of all, compared to high-T_c materials, MgB_2 is much more metallic, with very much lower resistivity, which results in a lower anisotropy. The low resistivity is especially beneficial to the noise properties in SQUIDs. Additionally, the *c*-axis coherence length in MgB_2 is about 5 nm, which is larger than in high-T_c superconductors (HTS). An advantage of longer coherence length materials in junctions is that the effect of a degraded layer with lower T_c near the electrode-barrier interface is reduced. The coherence length in the MgB_2 *a–b* plane is even larger, suggesting that *a–b* plane junctions are even more advantageous for applications.

Secondly, the critical temperature of 40 K of MgB_2 is attractive from a cooling point of view [4]. Superconducting rapid single flux quantum logic (RSFQ) circuitry is now typically based on low-T_c $Nb/Al_2O_3/Nb$ technology, which has to be cooled to 4–5 K. HTS oxide technology, on the other hand, allows for a higher operating temperature. However, due to bit-error rates at elevated temperatures, 20–30 K is generally regarded as the optimal operating temperature. In that sense, all-MgB_2 junctions are at least as attractive, avoiding the materials science issues that are still hampering HTS technology, and allowing the use of compact cryocoolers. For a heat load of 1 W the advantages of cooling to 25 K instead of 4.5 K are, for example, a volume reduction from 0.2 to 0.01 m^3 and an input power reduction from 1500 to 150 W [5].

A spread in junction properties, particularly I_c, of less than 2% is required in order to fabricate RSFQ circuitry with large numbers of junctions. This small spread has been achieved in $Nb/Al_2O_3/Nb$ technology, but has not yet been possible with HTS and is still a major challenge for MgB_2 junction technology.

Finally, the product of the critical current and the normal state resistance, I_cR_N for unshunted junctions, is predicted to be high compared to that of low-T_c materials [6], especially in the case of tunneling in the crystallographic MgB_2 *ab*-plane. The large energy gap of MgB_2 should also allow higher frequency operation of SIS detectors.

Parallel to the initial development of junctions and SQUIDs, the notion started to develop that MgB_2 is a model example of a multiband superconductor [7], with a comparable weight of the respective bands. This notion spurred a second urge for MgB_2 junctions, this time as devices for spectroscopic measurements of the electronic properties of MgB_2. The conductance through a superconductor–insulator–normal metal tunnel junction is proportional to the density of states in the superconductor, and an MgB_2–insulator–metal junction is, therefore, an ideal spectroscopic device, where the metal can either be a normal metal or a superconductor with a lower-critical temperature. Needless to say, that in order to probe the anisotropic transport properties of MgB_2, it is essential that the MgB_2 electrode is oriented. Oriented, or even in-plane epitaxial, devices also provide reproducibility advantages for all-MgB_2 Josephson junctions for RSFQ and SQUIDs for magnetic field sensing applications.

Here, we will review the state of the art of MgB_2 devices and describe recent advances in the realization of thin films, tunnel junctions (both for spectroscopic purposes as well as superconducting electronics) and SQUIDs. Finally, novel MgB_2 devices will be discussed, that are uniquely based on the multiband character of MgB_2.

2. Epitaxial thin films

The main requirements on thin films for most devices are a high and stable transition temperature (no degradation upon exposure to the environment and structuring), a smooth and dense morphology, and an oriented or even epitaxial crystal structure. The influence of the film density and grain connectivity on the transport properties was discussed by Rowell [8].

Films with very high and stable transition temperatures (39 K) have been obtained by means of ex-situ deposition techniques [9], in which a B film is typically exposed to a high-pressure Mg vapor at high temperatures, to let it react to MgB_2. However, the large surface roughness and low density of such films make these films unsuitable for most device applications.

In-situ MgB_2 film growth techniques (see Refs. [10–15] for early thin film results) deal with three major challenges. The first challenge lies in avoiding the oxidation of Mg and B, which generally requires very pure target materials and high-vacuum deposition conditions. The second complication is the large difference in vapor pressures of B and Mg, the Mg vapor pressure being orders of magnitude higher than that of B. Thirdly, the Mg sticking coefficient is very low above about 300 °C. Most growth methods are, therefore, limited to low temperatures, since not sufficient Mg can be provided at elevated temperatures, typically leading to films with a reduced T_c, enhanced resistivity as compared to bulk MgB_2 and a low degree of orientation.

Beneficially, the growth of MgB_2 is found to be kinetically and absorption limited [16], meaning that the Mg does not escape from the film after the right phase has formed during growth, and that the right phase will form as long as sufficient Mg vapor is present. A number of growth techniques explicitly benefit from these properties by independently tuning the B and Mg fluxes, or by simply providing a large excess of Mg flux. The independent flux tuning is used for example in combinations of pulsed-laser deposition of Mg with sputter-deposition of B [17], or e-beam evaporation of B with evaporation of Mg [13], or sputter-deposition of B with evaporation of Mg [18]. When the Mg vapor can be confined close to the film, as with a closed container, high quality eptiaxial films have recently been obtained [19,20].

The best epitaxial MgB_2 films in terms of high-T_c, low resistivity, smoothness, and degree of orientation have

been obtained by the hybrid physical chemical vapor deposition (HPCVD) method as developed at Pennsylvania State University [20] and described in detail in this issue. The B in the HPCVD method is supplied in the form of diborane gas, which is unfortunately not available in many laboratories. For reasons that are not understood, the films of Moeckly and Ruby [19] have the advantage of having a stable T_c upon exposure to air and moisture. To prevent degradation of other MgB_2 films, a passivation coating such as TaN can be used, that still allows for electrical contacts to be made [21].

3. Quasiparticle and Josephson tunnel junctions

3.1. Multiband transport

The multiband nature of superconductivity in MgB_2 is by now well established by a number of experiments and theoretical modeling [7]. MgB_2 has become an important two-band model system, also of importance to other multiband superconductors, and perhaps even to the high-T_c cuprates as well [22]. The two conduction bands of MgB_2 are usually referred to as the π- and the σ-band, following the labeling of Liu et al. [23]. The σ Fermi surface sheets originate from the σ-bonds in the hexagonal two-dimensional B lattice sheets, while the π Fermi surface sheets originate from the π bonding and antibonding between the Mg and B sheets. Consequently, the σ-band is almost two-dimensional, in the crystallographic a–b plane, while the π-band has more three-dimensional character. The qualitative difference between the Fermi surface sheets, combined with the large disparity of the electron–phonon coupling function, gives rise to two co-existing superconducting condensates below T_c.

The influence of the co-existence of two superconducting condensates on the transport properties of heterostructures is often far from trivial. An example is a two-band superconductor – normal metal bilayer, for which theory predicts [24] that the interplay between the proximity effect and the interband coupling influences the magnitudes of the superconducting gaps near the interface. Remarkably, this interplay can even give rise to an enhancement of the π and σ gaps when MgB_2 is in proximity with a superconductor with a lower transition temperature [24].

Another multiband transport phenomenon is the occurrence of multiple peaks in the conductivity spectrum of tunnel junctions. The contribution of the σ-band is especially pronounced when tunneling in the crystallographic MgB_2 a–b plane is considered, whereas the π-band has a more three-dimensional character [6]. Models to calculate the conductivity of tunnel junctions have recently been refined to take into account the specific shape of the Fermi surface of MgB_2 [25,26]. To illustrate the anisotropy of transport through metal–barrier–MgB_2 junctions, the example of a model calculation of a Au–insulator–MgB_2 junction is shown in Fig. 1. Here, the Fermi surface of Au is taken spherically and the π and σ sheets of the approximated MgB_2 Fermi surface [27] are sketched schematically. For tunneling into the crystallographic a–b plane direction, two peaks in the conductance spectrum clearly appear, while the σ-peak is only very weak for tunneling into the c-axis direction. The first and very clear

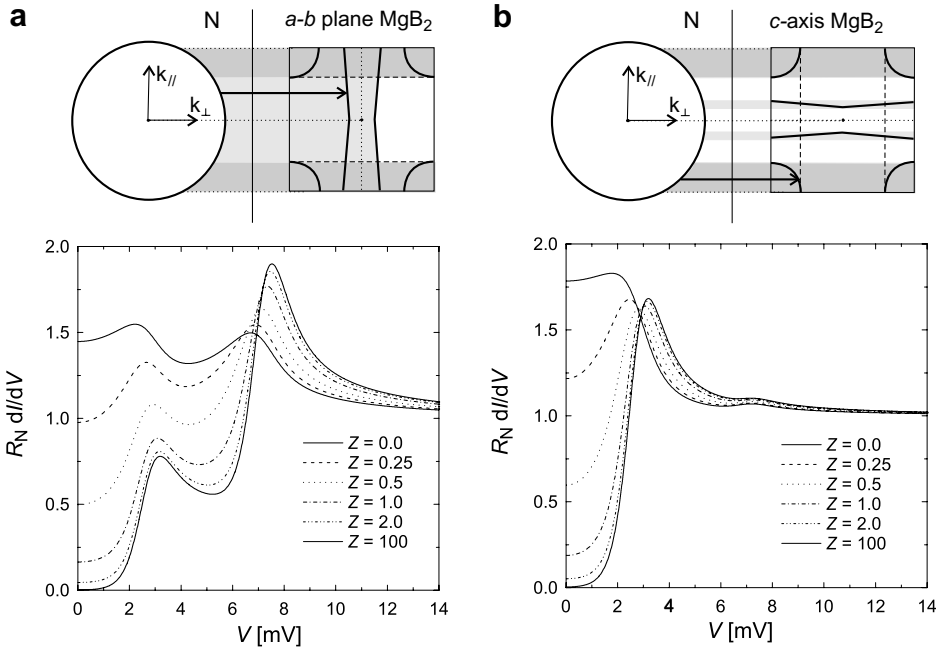

Fig. 1. (a) Normal metal – MgB_2 tunneling in the a–b plane direction for several interface transparencies [25], ranging from $Z = 0$ for Andreev contacts to $Z \gg 1$ for tunnel junctions. The barrier parameter Z is determined by the barrier potential U and the Fermi velocity v_F by $Z = U/\hbar v_F$. The normal metal Fermi surface is taken as a sphere, while the π and σ parts of the MgB_2 Fermi surface are approximated as in Ref. [27]. (b) Normal metal – MgB_2 tunneling in the c-axis direction for several interface transparencies, ranging from $Z = 0$ for Andreev contacts to $Z \gg 1$ for tunnel junctions.

experimental confirmation of these concepts was provided by the point-contact spectroscopy of Gonnelli et al. [28].

3.2. MgB_2–insulator–metal junctions

Apart from the point contact experiments on crystals, multilayer *c*-axis tunnel junctions have been realized as well that allow for a spectroscopic investigation of MgB_2 [29–38]. All of these studies confirm the existence of the small π gap, its value centering around 2.0–2.5 meV. The presence of the σ gap is not always resolved from the noise. Clear examples in which both the small π gap and a small signature of the σ gap are seen in the conductance of a *c*-axis MgB_2–insulator–metal tunnel junctions [34,37], are shown in Fig. 2a and b. The width of the sum-gap peak is usually wider than expected from carrier lifetime broadening due to temperature alone. This indicates that the gap is not always completely homogeneous close to the barrier, possibly due to degradation towards the interface.

In cases where the tunnel barrier provides tunnel junctions with high resistance, the energy region above the gap can be investigated as well, from which the electron–phonon coupling function α^2F can be obtained [39]. Geerk et al. [35] measured both the dI/dV and the d^2I/dV^2 spectrum up to high voltages of a *c*-axis MgB_2/oxide–insulator/In junction, providing insight into the phonons and the interband pairing interaction, see Fig. 2c. It should be realized that the inverse problem of obtaining α^2F from d^2I/dV^2 can be mathematically ill-defined in the multiband case [40].

High-quality MgB_2–insulator–metal junctions in the crystallographic *a*–*b* plane direction have not yet been achieved. In a ramp-type geometry closed (i.e. pinhole free) Al_2O_3 barriers were realized in an MgB_2–Al_2O_3–Nb junction, evidenced from an ideal supercurrent modulation as function of applied magnetic field [36]. However, despite the excellent Josephson properties, only very broad *a*–*b* plane spectra were obtained with very low gap values because of a degradation of the MgB_2 during the etching of the ramp. The realization of these type of junctions still is one of the challenges in the field.

3.3. Suitable barrier materials for all-MgB_2 Josephson junctions

Several materials have proven to be useful as the barrier in MgB_2–insulator–metal junctions, of which oxidized Al and AlN are most often used [30,32–34,36], while oxidation of the MgB_2 film itself has also been shown to make good tunnel barriers [35,38]. The restrictions on the use of materials as the tunnel barrier in junctions with two MgB_2 electrodes are more stringent than in MgB_2–insulator–metal junctions, since a high-temperature (typically >300 °C) MgB_2 deposition step is required after barrier deposition. The realization of reproducible all-MgB_2 junctions is still proving to be a major challenge.

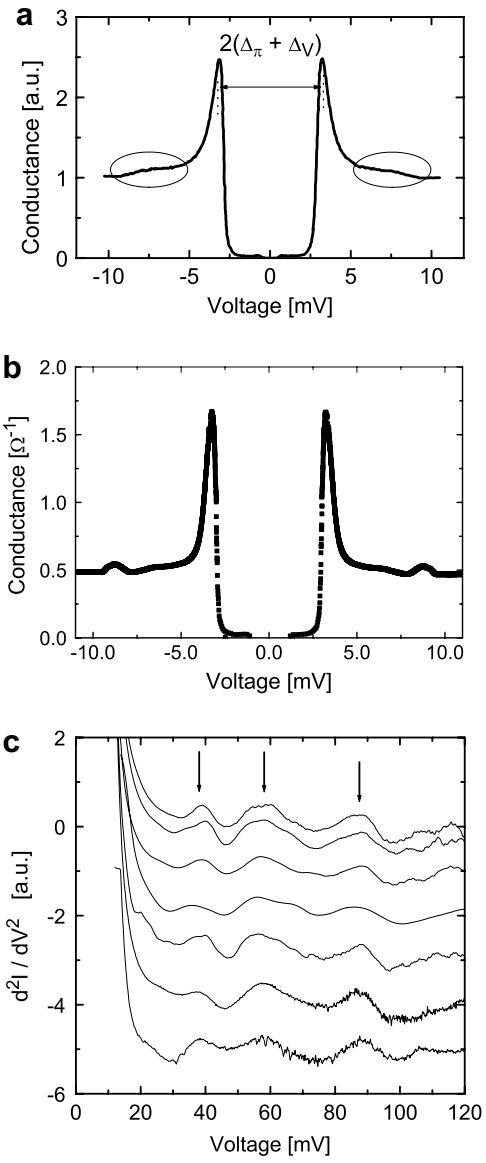

Fig. 2. (a) Differential resistance of the *c*-axis MgB_2–Al_2O_3–V junction of Kim et al. [34], at 0.5 K. The π as well as the σ gaps (and the difference with the V gap) are as theoretically predicted in Fig. 1b. (b) Differential resistance of a *c*-axis MgB_2–insulator–Pb junction from Cui et al. [37], at 4.3 K, also clearly showing the σ gap. The MgB_2 in this case was made with HPCVD. (c) d^2I/dV^2 second-derivative tunnel spectra of the six different *c*-axis MgB_2–oxide–In junctions of Geerk et al. [35]. The upper two traces are taken on the same junction, with positive and negative voltage bias. The In counterelectrode is driven normal by a magnetic field of 0.1 T.

The most logical alternatives to trilayer MgB_2 junctions are in-plane junctions with some type of restriction or region of depressed T_c. It is known that the T_c of MgB_2 can be monotonically reduced by irradiation either by ions [21] or by neutrons [41], making it a useful way of realizing weak links. Such in-plane junctions have been realized in a variety of ways, such as by locally reducing the thickness [42,43], by local ion damage [44,45], by transport through normal metals [44,46] or proximized TiB_2 [47]. The latter result is a promising route towards all-boride SNS junctions,

but ion milling inhomogeneities are still hampering the junction reproducibility.

One of the earliest barrier materials that was used in all-MgB_2 multilayer ramp type junctions was MgO [2]. MgO barriers (made by the oxidation of a thin film of Mg) are known to survive high temperature deposition steps in MRAM technology, where very small spreads of R_N have been achieved. Ramp type junctions have the advantage of having a tunneling component in the *a–b* plane direction. When no barrier was deposited before the deposition of the counter electrode, a strong superconducting link was observed, indicating that the etching of the ramp does not completely destroy the superconductivity in MgB_2. All junctions with MgO barriers showed RSJ-like characteristics, albeit with a small amount of non-Josephson supercurrent, indicating that the barrier was not completely pinhole free [2].

Closed tunnel barriers in all-MgB_2 *c*-axis trilayer junctions were obtained by Shimakage et al. with AlN as the barrier material [48] and by Ueda et al. with an Al_2O_3 barrier [49,50]. Both groups were able to measure the sum-gap voltage $2\Delta_\pi$ and to obtain a near-ideal critical current modulation by applied magnetic field. No reproducibility numbers have been provided yet for these promising tunnel junctions.

The transport properties of the MgB_2–AlN–MgB_2 junctions have been determined for a range of barrier thicknesses. Tunneling is observed down to very small amounts of deposited AlN, indicating that in addition to the AlN, some form of natural oxide is also present as the barrier, perhaps even in the form of a degraded first or second layer. The presence of some form of degradation of MgB_2 in the electrodes is supported by the lack of supercurrent above about 20 K in the AlN and Al_2O_3 junctions [48,49], while the gaps are observed to higher temperatures. Multiband tunneling models [6] predict an inflection point in the *c*-axis supercurrent as a function of temperature around 20 K, but it does not completely vanish, as can be seen in Fig. 3a. It is interesting to study further whether the absence of supercurrent above 20 K in *c*-axis tunnel junctions (see Fig. 3b) is due to degradation or some aspect of multiband superconductivity.

The native oxide has also been studied as the barrier material by varying the film deposition conditions, its surface stoichiometry, and the oxidation temperature. As is the case for MgB_2–oxide–In junctions [35], in all-MgB_2 junctions, the native oxide also provides a very thick tunnel barrier [51]. The native oxide barrier is typically so thick that hardly any supercurrent is observed, but the junctions are suitable for spectroscopic purposes.

4. SQUIDs and magnetometers

The fact that no ideal all-MgB_2 multilayer Josephson junctions have been demonstrated yet has not hampered the development of thin film magnetic field sensing devices. A nano-constriction with a size smaller than the London penetration depth or a region of lower-T_c can act as a weak link as well and develop a current-phase relation, which is sufficient for observing superconducting quantum interference.

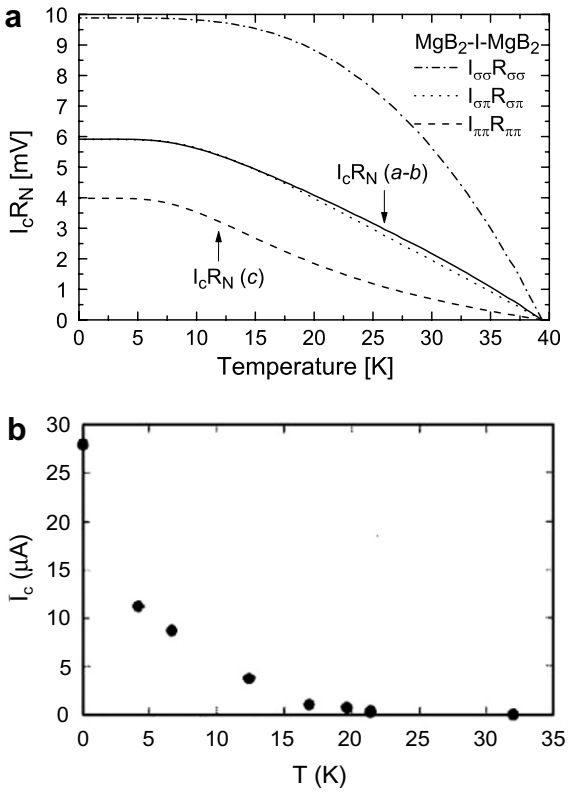

Fig. 3. (a) Model results [6] for the temperature dependence of the normalized critical Josephson current from one band (σ or π) to the other (σ or π) of MgB_2–I–MgB_2 tunnel junctions, where the normalization factor R_N is constant as function of temperature. The total junction's supercurrent depends on the orientation. The results for tunneling into the *c*-axis and *a–b* plane directions are indicated. (b) Experimental temperature dependence of the critical current in a *c*-axis MgB_2–Al_2O_3–MgB_2 junction, taken from Ref. [49].

The first MgB_2 SQUID [3] was based on such nano-constrictions. Two nano-constrictions in a loop were focused-ion beam etched in a pulsed-laser deposited MgB_2 film, thereby forming a SQUID. Soon after, the Berkeley group [52] reported an MgB_2 SQUID based on tunable point contacts in polycrystalline bulk material. Although the method used is not very suitable for applications, the reported noise value for an optimally tuned SQUID ($\beta_L \simeq 1$) of 35 fT $Hz^{-1/2}$ above 500 Hz at 19 K is promising. Burnell et al. [53] realized MgB_2 SQUIDs with weak links operating up to 20 K by locally degrading the superconducting properties of MgB_2 through focused ion beam irradiation. The obtained voltage modulation is large and the white flux noise of $14\mu\Phi_0$ $Hz^{-1/2}$ is comparable to noise levels in high-T_c SQUIDs.

To benefit more fully from the properties of MgB_2 (high-T_c, low resistivity, and multiband transport), SQUIDs have recently been realized on clean and epitaxial HPCVD MgB_2 films [54]. The nano-bridge dimensions are

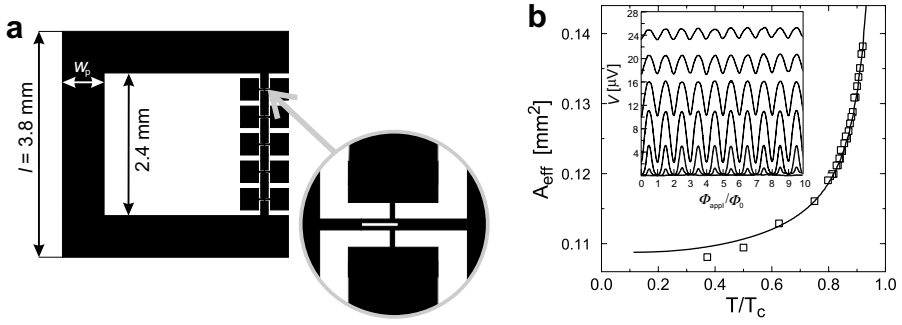

Fig. 4. (a) SQUID magnetometer design. An inductively coupled pick-up loop enhances the effective area of the SQUID. The SQUID loop itself is shown in the magnified inset. The weak links are formed by focused-ion-beam etching two nano-constrictions in the SQUID loop. (b) The measured effective MgB_2 magnetometer area is a function of temperature due to the kinetic inductance of the striplines in the SQUID loop. This temperature dependence can be well explained by taking the multiband character of the superconducting penetration depth into account [54]. The inset shows the voltage modulation of a single-crystalline MgB_2 SQUID under applied magnetic flux for several values of the current bias at an operating temperature of 37 K.

much smaller than the typical grain sizes in the film, so that true single-crystal behavior could be observed. A large critical current density of 5×10^7 A/cm^2 at 4.2 K, and stable SQUID voltage modulation up to 38.8 K was observed. The voltage modulation of the SQUID is shown in the inset of Fig. 4b at a temperature of 37 K for several values of the bias current.

An inductively shunted magnetometer was designed as depicted in Fig. 4a. The inductive shunt enhances the effective SQUID area, while keeping its inductance small. As described in Ref. [54], the effective area is a function of the kinetic inductance of the striplines and, therefore, a function of the MgB_2 penetration depth. The measured effective area of the magnetometer is shown in Fig. 4b and could not be fitted with the standard expressions for the penetration depth. This can be explained from the fact that the penetration depth in MgB_2 arises from two bands.

Qualitatively, in clean multiband systems, the low temperature dependence is determined by the π-band with the smallest gap, whereas the high temperature behavior results from the σ-band with the larger gap, giving an inflection point in the penetration depth temperature dependence. On the other hand, when the superconducting π-band is 'overdamped' due to impurities, then the penetration depth is only determined by the σ-band and it will show a BCS temperature dependence. When the multiband nature is taken into account with a microscopic model [55] based on the Eliashberg formalism and the results of first principles electronic structure calculations, the magnetometer behavior could be explained in terms of clean transport in the crystallographic a–b plane direction. The obtained value for $\lambda(0) = 62$ nm is very close to the theoretical predictions [55], but much smaller than had been measured so far, since for the first time clean and epitaxial films have been used. The clean and multiband nature of these HPCVD films has been confirmed by a study of their magnetoresistance recently [56].

The MgB_2 magnetometer white noise level was measured [54] to be $S_\phi^{1/2}(\nu) = 76\mu\Phi_0\ \mathrm{Hz}^{-1/2}$ and below 1 Hz the noise appears with a magnitude proportional to $1/\nu^2$. The effective magnetic field noise $S_B^{1/2}(\nu) = S_\phi^{1/2}(\nu)/A_{\mathrm{eff}} = 1\ \mathrm{pT\ Hz}^{-1/2}$. Despite the fact that single-crystalline MgB_2 has weaker flux-pinning properties than polycrystalline samples [57], the obtained noise value indicates that this does not pose any problems. The obtained magnetometer noise value is promising for a device that has not yet been optimized. For HTS magnetometers, lower noise values were reported, but these were fabricated on larger samples (1–4 cm^2). Using larger MgB_2 samples, the magnetic field noise level in inductively shunted dc SQUIDs is expected to be reduced as well. Progress in obtaining large area magnetometers was recently reported by Portesi et al. [58]. An alternative route to reduce noise is to study and manipulate the pinning of vortices in the films. This topic is heavily studied for large scale applications as well, as discussed in this issue.

5. Novel multiband phase devices

In 1966, A.J. Leggett predicted for a hypothetical two-band superconductor, the existence of a collective excitation, corresponding to small fluctuations of the relative phase of the two condensates [59]. More recently, these results were applied to MgB_2 by Sharapov et al. [60] using an effective action approach. Estimates for the mode energy for the case of MgB_2 vary from 6.5 to 8.9 meV, depending on the calculated coupling constants.

In a junction consisting of a two-band and a one-band superconductor, an additional contribution to the dc current is expected, when the voltage across the junction matches the energy of the Leggett mode [61]. In that case, the ac Josephson effect between the one-band superconductor and the mean phase of the two-band superconductor serves as a driving force for the interband oscillation in the two-band superconductor. Since at this specific voltage the frequencies of the two oscillations are equal, a net dc current through the junction will arise. Some first indications exist that this effect might have been observed [25,62,63] in MgB_2 junctions. More detailed investigations on high-quality a–b plane junctions are necessary to explore this intriguing effect.

When it is indeed confirmed that the phases of the two superconducting condensates in a two-band superconductor are not necessarily equal, the phase difference can be used in devices as an additional internal degree of freedom, that can carry information. Interesting is the possibility for an interband sign reversal of the order parameter (i.e. a spontaneous π-shift between the phases of the superconducting wave functions in different parts of the Fermi surface). This is expected to be possible [61,64], but the conditions for this effect have not yet been studied in detail. Spontaneous phase shifts attracted recently much interest since they may be used to create the so-called Josephson π-junction, which exhibits a spontaneous phase π-shift in the ground state.

A different mechanism of creating a difference between the phases of the two superconducting bands can be imagined. In analogy with the multiband proximity effect [24], one can use the non-equilibrium effect of a current flow perpendicular to a normal metal (or single-band superconductor) – multiband superconductor interface as the means of creating a phase difference between the superconducting bands. The existence of phase shifts should lead to interband currents, i.e. a kind of intrinsic Josephson effect, comparable to the widely studied intrinsic Josephson effect in high-T_c superconductors.

6. Conclusion

Despite the very early initial exploration of MgB_2 for electronic circuitry, still no completely reproducible all-MgB_2 Josephson junction technology with low I_c spreads is available. But the high-quality devices for measuring MgB_2 spectra, as well as recent advances in trilayer junctions and detailed studies of barrier materials and their epitaxy with MgB_2 films are promising and should be pursued further. For RSFQ applications, a reliable MgB_2 technology could boost superconducting electronic applications cooled by cryocoolers.

The multiband character of the superconductivity is explored in MgB_2–insulator–metal tunnel junctions and has helped to understand two-band superconductivity and has led to novel phenomena such as phase resonances and double peaks in the conductivity. The multiband nature of superconductivity in MgB_2 could even lead to novel types of non-equilibrium devices based on the phase degrees of freedom of the two condensates.

Multiband properties even show up in the transport characteristics of MgB_2 magnetometers. It was found that the latter does not hamper their correct operation. Reliable SQUIDs and low-noise magnetometers have been realized that operate close to the T_c of MgB_2.

Acknowledgements

We thank our colleagues at the University of Twente, Arizona State University, Pennsylvania State University, the Massachusetts Institute for Technology, Superconductor Technologies Inc., the IEN Torino, and the Politecnico di Torino for fruitful collaborations.

References

[1] J. Nagamatsu, N. Nakagawa, T. Muranaka, Y. Zenitani, J. Akimitsu, Nature 410 (2001) 63.
[2] D. Mijatovic, A. Brinkman, I. Oomen, G. Rijnders, H. Hilgenkamp, D.H.A. Blank, H. Rogalla, Appl. Phys. Lett. 80 (2001) 2141.
[3] A. Brinkman, D. Veldhuis, D. Mijatovic, G. Rijnders, D.H.A. Blank, H. Hilgenkamp, H. Rogalla, Appl. Phys. Lett. 79 (2001) 2420.
[4] J.M. Rowell, Nature Mater. 1 (2002) 5.
[5] H.J.M. ter Brake, F.-Im. Buchholz, G. Burnell, T. Claeson, D. Crété, P. Febvre, G.J. Gerritsma, H. Hilgenkamp, R. Humphreys, Z. Ivanov, W. Jützi, M.I. Khabipov, J. Mannhart, H.-G. Meyer, J. Niemeyer, A. Ravex, H. Rogalla, M. Russo, J. Satchell, M. Siegel, H. Töpfer, F.H. Uhlmann, J.-C. Villégier, E. Wikborg, D. Winkler, A.B. Zorin, Physica C 439 (2006) 1.
[6] A. Brinkman, A.A. Golubov, H. Rogalla, O.V. Dolgov, J. Kortus, Y. Kong, O. Jepsen, O.K. Andersen, Phys. Rev. B 65 (2002) 180517.
[7] Physica C 385 (1–2) (2003) (special issue on MgB_2).
[8] J.M. Rowell, Supercond. Sci. Technol. 16 (2003) R17.
[9] W.N. Kang, H.J. Kim, E.M. Choi, C.U. Jung, S.L. Lee, Science 292 (2001) 1521.
[10] D.H.A. Blank, H. Hilgenkamp, A. Brinkman, D. Mijatovic, G. Rijnders, H. Rogalla, Appl. Phys. Lett. 79 (2001) 394.
[11] W. Jo, J.U. Huh, T. Ohnishi, A.F. Marshall, M.R. Beasley, R.H. Hammond, Appl. Phys. Lett. 80 (2002) 3563.
[12] K. Ueda, M. Naito, Appl. Phys. Lett. 79 (2001) 2046.
[13] A. Erven, T.H. Kim, M. Muenzenberg, J.S. Moodera, Appl. Phys. Lett. 81 (2002) 4982.
[14] J. Kim, R.K. Singh, N. Newman, J.M. Rowell, IEEE Trans. Appl. Supercond. 13 (2003) 3238.
[15] E. Monticone, C. Gandini, C. Portesi, M. Rajteri, S. Bodoardo, N. Penazzi, V. Dellarocca, R.S. Gonnelli, Supercond. Sci. Technol. 17 (2004) 649.
[16] Z.Y. Fan, D.G. Hinks, N. Newman, J.M. Rowell, Appl. Phys. Lett. 79 (2001) 87.
[17] D. Mijatovic, A. Brinkman, H. Hilgenkamp, H. Rogalla, G. Rijnders, D.H.A. Blank, Appl. Phys. A – Mater. Sci. Process. 79 (2004) 1243.
[18] R. Schneider, J. Geerk, F. Ratzel, G. Linker, A.G. Zaitsev, Appl. Phys. Lett. 85 (2004) 5290.
[19] B.H. Moeckly, W.S. Ruby, Supercond. Sci. Technol. 19 (2006) L21.
[20] X.H. Zeng, A.V. Progrebnyakov, A. Kotcharov, J.E. Jones, X.X. Xi, E.M. Lysczek, J.M. Redwing, S.Y. Xu, Q. Li, J. Lettieri, D.G. Schlom, W. Tian, X.Q. Pan, Z.K. Liu, Nature Mater. 1 (2002) 1.
[21] R. Gandikota, R.K. Singh, J. Kim, J.M. Rowell, N. Newman, B. Wilkens, A.V. Pogrebnyakov, X.X. Xi, Appl. Phys. Lett. 86 (2005) 012508.
[22] A. Brinkman, H. Hilgenkamp, Physica C 422 (2005) 71.
[23] A.Y. Liu, I.I. Mazin, J. Kortus, Phys. Rev. Lett. 87 (2001) 087005.
[24] A. Brinkman, A.A. Golubov, M.Yu. Kupriyanov, Phys. Rev. B 69 (2004) 214407.
[25] A. Brinkman, S.H.W. Van der Ploeg, A.A. Golubov, H. Rogalla, T.H. Kim, J.S. Moodera, J. Phys. Chem. Solids 67 (2006) 407.
[26] T. Dahm, N. Schopol, Phys. Rev. B 74 (21) (2006).
[27] T. Dahm, N. Schopol, Phys. Rev. Lett. 91 (2003) 17001.
[28] R.S. Gonnelli, D. Daghero, G.A. Ummarino, V.A. Stepanov, J. Jun, S.M. Kazakov, J. Karpinski, Phys. Rev. Lett. 89 (2002) 247004.
[29] M.H. Badr, M. Freamat, Y. Sushko, K.W. Ng, Phys. Rev. B 65 (2002) 184516.
[30] G. Carapella, N. Martuciello, G. Costabile, C. Ferdeghini, V. Ferrando, G. Grassano, Appl. Phys. Lett. 80 (2002) 2949.
[31] A. Saito, A. Kawakami, H. Shimakage, T.H. Terai, Z. Wang, IEEE Trans. Appl. Supercond. 13 (2003) 1067.
[32] K. Ueda, M. Naito, IEEE Trans. Appl. Supercond. 13 (2003) 3249.
[33] Shimakage et al., Supercond. Sci. Technol. 17 (2004) 1376.

[34] T.H. Kim, J.S. Moodera, Appl. Phys. Lett. 85 (2004) 434.
[35] J. Geerk, R. Schneider, G. Linker, A.G. Zaitsev, R. Heid, K.-P. Bohnen, H.V. Lohneysen, Phys. Rev. Lett. 94 (2005) 227005.
[36] M. van Zalk, A. Brinkman, A.A. Golubov, H. Hilgenkamp, T.H. Kim, J.S. Moodera, H. Rogalla, Supercond. Sci. Technol. 19 (2006) S226.
[37] Y. Cui, K. Chen, Q. Li, X.X. Xi, J.M. Rowell, IEEE Trans. Appl. Supercond., in press.
[38] Y. Cui, K. Chen, Q. Li, X.X. Xi, J.M. Rowell, Appl. Phys. Lett. 89 (2006) 202513.
[39] W.L. McMillan, J.M. Rowell, in: R.D. Parks (Ed.), Superconductivity, vol. 1, Dekker, New York, 1969, p. 561.
[40] O.V. Dolgov, R.S. Gonnelli, G.A. Ummarino, A.A. Golubov, S.V. Shulga, J. Kortus, Phys. Rev. B 68 (2003) 132503.
[41] M. Putti, M. Affronte, C. Ferdeghini, P. Manfrinetti, C. Tarantini, E. Lehmann, Phys. Rev. Lett. 96 (2006) 077003.
[42] G. Burnell, D.-J. Kang, H.N. Lee, S.H. Moon, B. Oh, M.G. Blamire, Appl. Phys. Lett. 79 (2001) 3464.
[43] D.A. Kahler, J. Talvacchio, J.M. Murduck, A. Kirschen-baum, R.E. Brooks, S.B. Bu, J. Choi, D.M. Kim, C.-B. Eom, IEEE Trans. Appl. Supercond. 13 (2003) 1063.
[44] D.-J. Kang, N.H. Peng, R. Webb, C. Jeynes, J.H. Yun, S.H. Moon, B. Oh, G. Burnell, E.J. Tarte, D.F. Moore, M.G. Blamire, Appl. Phys. Lett. 81 (2002) 3600.
[45] S.A. Cybart, K. Chen, Y. Cui, Q. Li, X.X. Xi, R.C. Dynes, Appl. Phys. Lett. 88 (2006) 012509.
[46] J.I. Kye, H.N. Lee, J.D. Park, S.H. Moon, B. Oh, IEEE Trans. Appl. Supercond. 13 (2003) 1075.
[47] K. Chen, Y. Cui, Q. Li, X.X. Xi, S.A. Cybart, R.C. Dynes, X. Weng, E.C. Dickey, J.M. Redwing, Appl. Phys. Lett. 88 (2006) 222511.
[48] H. Shimakage, K. Tsujimoto, Z. Wang, M. Tonouchi, Appl. Phys. Lett. 86 (2005) 072512.
[49] K. Ueda, S. Saito, K. Semba, T. Makimoto, M. Naito, Appl. Phys. Lett. 86 (2005) 172502.
[50] K. Ueda, M. Naito, IEICE Trans. Electron. 88 (2005) 226.
[51] R.K. Singh, R. Gandikota, J. Kim, N. Newman, J.M. Rowell, Appl. Phys. Lett. 89 (2006) 042512.
[52] Y. Zhang, D. Kinion, J. Chen, J. Clarke, D.G. Hinks, G.W. Crabtree, Appl. Phys. Lett. 79 (2001) 3995.
[53] G. Burnell, D.-J. Kang, D.A. Ansell, H.-N. Lee, S.-H. Moon, E.J. Tarte, M.G. Blamire, Appl. Phys. Lett. 81 (2002) 102.
[54] D. Mijatovic, A. Brinkman, D. Veldhuis, H. Hilgenkamp, H. Rogalla, G. Rijnders, D.H.A. Blank, A.V. Pogrebnyakov, J.M. Redwing, S.Y. Xu, Q. Li, X.X. Xi, Appl. Phys. Lett. 87 (2005) 192505.
[55] A.A. Golubov, A. Brinkman, O.V. Dolgov, J. Kortus, O. Jepsen, Phys. Rev. B 66 (2002) 054524.
[56] Q. Li, B.T. Liu, Y.F. Hu, J. Chen, H. Gao, L. Shan, H.H. Wen, A.V. Progrebnyakov, J.M. Redwing, X.X. Xi, Phys. Rev. Lett. 96 (2006) 167003.
[57] A.K. Pradhan, M. Tokunaga, K. Yamazaki, T. Tamegai, Y. Takano, K. Togano, H. Kito, H. Ihara, Phys. Rev. B 68 (2003) 104514.
[58] C. Portesi, D. Mijatovic, D. Veldhuis, A. Brinkman, E. Monticone, R.S. Gonnelli, Supercond. Sci. Technol. 19 (2006) S303.
[59] A.J. Leggett, Prog. Theor. Phys. 36 (1966) 901.
[60] S.G. Sharapov, V.P. Gusynin, H. Beck, Eur. Phys. J. B 30 (2002) 45.
[61] D.F. Agterberg, E. Demler, B. Janko, Phys. Rev. B 66 (2002) 214507.
[62] Ya.G. Ponomarev et al., Solid State Commun. 129 (2004) 85.
[63] Ya.G. Ponomarev et al., Pis'ma ZhETF 79 (2004) 597.
[64] A.A. Golubov, I.I. Mazin, Phys. Rev. B 55 (1997) 15146;
I.I. Mazin, A.A. Golubov, A.D. Zaikin, Phys. Rev. Lett. 75 (1995) 2574.